JOURNAL OF VIROLOGY, Nov. 2007, p. 12029–12039 Vol. 81, No. 21
0022-538X/07/$08.00+0 doi:10.1128/JVI.00315-07

Specific Asparagine-Linked Glycosylation Sites Are Critical for DC-SIGN- and L-SIGN-Mediated Severe Acute Respiratory Syndrome Coronavirus Entry▽

Dong P. Han,[1] Motashim Lohani,[1] and Michael W. Cho[1,2,3]*

Departments of Medicine,[1] Biochemistry,[2] and Molecular Biology and Microbiology,[3] Case Western Reserve University School of Medicine, Cleveland, Ohio 44106

Received 12 February 2007/Accepted 11 August 2007

Severe acute respiratory syndrome (SARS) is caused by a newly emerged coronavirus (CoV) designated SARS-CoV. The virus utilizes angiotensin-converting enzyme 2 (ACE2) as the primary receptor. Although the idea is less clear and somewhat controversial, SARS-CoV is thought to use C-type lectins DC-SIGN and/or L-SIGN (collectively referred to as DC/L-SIGN) as alternative receptors or as enhancer factors that facilitate ACE2-mediated virus infection. In this study, the function of DC/L-SIGN in SARS-CoV infection was examined in detail. The results of our study clearly demonstrate that both proteins serve as receptors independently of ACE2 and that there is a minimal level of synergy between DC/L-SIGN and ACE2. As expected, glycans on spike (S) glycoprotein are important for DC/L-SIGN-mediated virus infection. Site-directed mutagenesis analyses have identified seven glycosylation sites on the S protein critical for DC/L-SIGN-mediated virus entry. They include asparagine residues at amino acid positions 109, 118, 119, 158, 227, 589, and 699, which are distinct from residues of the ACE2-binding domain (amino acids 318 to 510). Amino acid sequence analyses of S proteins encoded by viruses isolated from animals and humans suggest that glycosylation sites N227 and N699 have facilitated zoonotic transmission.

The etiological agent of severe acute respiratory syndrome (SARS) has been identified as a novel coronavirus (CoV) designated SARS-CoV (9, 20, 32, 35). SARS-CoV represents one of several pathogens that have emerged in recent years. The SARS epidemic during 2002 and 2003 had a major socioeconomic impact globally. Although SARS-CoV infections have not been reported recently, there is potential for the virus to reemerge in the future, considering that humans often come into contact with animals that are susceptible to virus infection or that serve as reservoirs (11, 21, 29). Better understanding of the mechanism(s) of virus entry into host cells could facilitate development of a vaccine and antiviral agents.

The entry of CoVs into cells is mediated by spike (S) glycoprotein. S protein of SARS-CoV is 1,255 amino acids (aa) long. It has a 13-aa signal peptide, a single ectodomain (1,182 aa), and a transmembrane region followed by a short cytoplasmic tail (28 residues) (28, 37). Although S proteins of many CoVs are cleaved into and function as two separate subunits, S1 and S2 (1, 17, 31), S protein of SARS-CoV is not (12, 47). It is presumed, nevertheless, to have two functional domains, and the border between them has been suggested to be around aa 680 (27, 41). The S1 domain is responsible for binding to cellular receptors, and the S2 domain contains two heptad repeat regions (HR1 and HR2) that form six-helix bundles (5, 16, 43, 50, 51) and mediate fusion between viral and cellular membranes.

The receptor for SARS-CoV has been identified as angiotensin-converting enzyme-related carboxypeptidase (ACE2) (24). The receptor-binding domain (RBD) has been narrowed down to amino acid residues 318 to 510 (3, 46, 47). A cocrystal structure of ACE2 bound to the RBD revealed that residues 424 to 494 form the receptor-binding motif (RBM) that directly contacts ACE2 (25). Not surprisingly, site-directed mutagenesis studies have identified many residues within this region as critical to binding ACE2 (6, 46).

Although it is clear that ACE2 serves as a receptor for SARS-CoV, other reports show that DC-SIGN (*d*endritic *c*ell-*s*pecific *I*CAM-3-*g*rabbing *n*onintegrin) and L-SIGN (for liver/lymph node-specific; also called CD209L or DC-SIGNR) also are involved in virus entry (18, 30, 48). DC-SIGN and L-SIGN (collectively referred to as DC/L-SIGN) are members of a C-type lectin family, the interactions of which with ligands are carbohydrate dependent (2, 14, 26); they specifically recognize high-mannose glycans (10). The exact role of these molecules in viral infection/pathogenesis is unclear and somewhat controversial. While one study reported that L-SIGN can serve as an alternative receptor (18), another study showed that DC/L-SIGN enhance only ACE2-mediated infections (30). Regardless, the potential role of DC/L-SIGN in SARS-CoV pathogenesis is great, since dendritic cells have been shown to transfer infectious viruses to susceptible target cells via DC-SIGN (48). Moreover, L-SIGN is expressed in human lung tissue on type II alveolar cells, which are important targets for SARS-CoV infection (8, 42). However, results from genetic analyses seem to suggest that homozygosity for L-SIGN plays a protective role in SARS-CoV infection by promoting higher levels of proteasome-mediated virus degradation (7). In light of these conflicting observations, the role of DC/L-SIGN in SARS-CoV infections needs to be further examined.

In this study, SARS pseudoviruses were utilized to charac-

* Corresponding author. Mailing address: Case Western Reserve University School of Medicine, Department of Medicine, Division of Infectious Diseases, 10900 Euclid Ave., Cleveland, OH 44106-4984. Phone: (216) 368-1221. Fax: (216) 368-0069. E-mail: mcho@case.edu.
▽ Published ahead of print on 22 August 2007.

TABLE 1. Primers used for generating mutant S glycoproteins[a]

Amino acid position of Asn	Sense-strand sequence (5′ to 3′)
29	gat gtt caa gct cct **CaG** tac act caa cat ac
65	ctt cca ttt tat tct **CaG** gtt aca ggg ttt c
73	ggg ttt cat act att **CaG** cat acg ttt ggc aac
109	gg gtt ttt gg**A** tc**C** acc atg aac **CaG** aag tca cag tcg gtg
118	cg gtg att att att **CaG** aat tct act aat g
119	gtg att att att aac **CaG** tct act aat gtt g
158	c gat aat gca ttt **CaG** tgc act ttc gag tac
227	g cct ctt ggt att **CaG** att aca aat ttt ag
269	ctc aag tat gat gaa **CaG** ggt aca atc aca g
318	gtt gtg aga ttc cct **CaG** att aca aac ttg tg
330	gga gag gtt ttt **CaG** gct act aaa ttc cc
357	c tct gtg ctc tac **CaG** tc**G** aca ttt ttt tca acc
589	agt gta att aca cc**C** gg**G** aca **CaG** gct tca tct gaa gtt gct gtt c
602	cta tat caa gat gtt **CaG** tgc act gat gtt tct
691	tca att gct tac tct **CaG** aac acc att gct ata
699	att gct ata cct act **CaG** ttt tca att agc att
783	acc cca act tt**T** aaa tat ttt ggt ggt ttt **CaG** ttt tca caa ata tta

[a] Capital letters indicate mutated nucleotides. Antisense primers are complementary to the sense primers. Bold type indicates where changes were made. In case of an amino acid change, the entire codon is boldfaced.

terize and to compare virus infections mediated by DC/L-SIGN and by ACE2. Here, we demonstrate unambiguously that DC/L-SIGN indeed serve as receptors for SARS-CoV and that they function independently of ACE2. As expected, glycans on S protein play an important role in DC/L-SIGN-mediated infections. Moreover, site-directed mutagenesis analyses revealed that carbohydrate moieties on specific asparagine (N)-linked glycosylation sites are critical. The results of our study provide a better understanding of SARS-CoV entry and identify another potential target for development of antiviral agents against the virus.

MATERIALS AND METHODS

Plasmids and site-directed mutagenesis. A plasmid encoding full-length wild-type human ACE2 was generously provided by Michael Farzan (24). Plasmids encoding DC-SIGN or L-SIGN (33, 34) were obtained from the NIH AIDS Research and Reference Reagent Program (catalog nos. 5444 and 6746, respectively). Site-directed mutagenesis of SARS-CoV S protein (pHCMV-S) (12) was performed using a QuikChange XL site-directed mutagenesis system (Stratagene) with *PfuTurbo* DNA polymerase. Seventeen pairs of primers were used to generate mutants. Sense-strand primer sequences are shown in Table 1. Some primers included silent mutations for introducing restriction sites. All of the mutations were verified by sequencing.

Pseudovirus production and infections. Cell lines TELCeB6 (38), HeLa, and Vero E6 were maintained in Dulbecco's modified Eagle's medium (DMEM) supplemented with 5 to 7% fetal bovine serum, 2 mM L-glutamine, and penicillin-streptomycin antibiotics. Cells were cultured in 5% CO_2 incubators at 37°C. Pseudoviruses that encode β-galactosidase were produced as we have previously described (12). Briefly, TELCeB6 cells, which continuously release murine leukemia virus particles, were cotransfected with plasmids encoding S glycoprotein (pHCMV-S) and pcDNA3.1 (Invitrogen) using Lipofectin (Invitrogen) per the manufacturer's protocol. To generate TELCeB6 cells that stably express S glycoprotein, cotransfected cells were selected in the growth medium containing Geneticin (0.4 μg/ml; Invitrogen). Geneticin-resistant clones were isolated and expanded, and those able to produce high titers of SARS pseudoviruses were selected. Although cells subsequently were maintained in the absence of Geneticin, they continuously produced pseudoviruses with titers of 5×10^3 to 6×10^3 per ml. The virus titer was determined in Vero E6 cells. Mutant pseudoviruses were produced by transient transfections with plasmids encoding mutant S proteins.

Pseudovirus infections were done using Vero E6 cells (96-well plates) or HeLa cells (24-well plates) transfected with plasmid encoding ACE2, DC-SIGN, or L-SIGN. Cells were transfected with 1 μg (or indicated amounts) of plasmid DNA per well using Lipofectin. After overnight incubation, culture medium was replaced. Approximately 24 h posttransfection, cells were infected with 100 to 150 infectious units of pseudoviruses. Pseudoviruses were allowed to adsorb onto cells for about 60 min. Cells subsequently were washed with serum-free DMEM to remove unadsorbed viruses, and fresh medium was added. Infections were allowed to proceed for an additional 1.5 days, at which time infected cells were stained with 5-bromo-4-chloro-3-indolyl-β-D-galactopyranoside and quantified as previously described (12). Unless specified, results of virus infections are shown as absolute titers (i.e., number of infectious foci) or normalized as a percentage of the wild-type control or no inhibitor (or neutralizing antibodies) for the given receptor.

Pseudovirus inhibition and neutralization assays. ACE2-derived inhibitory peptide P6 was previously described (13). The peptide or mannan (Sigma-Aldrich), dissolved in phosphate-buffered saline at the indicated concentrations, was preincubated with 100 infectious units of SARS-CoV pseudoviruses for 20 min at 37°C. Subsequently, the virus-inhibitor mixture was added to HeLa cells transfected with either ACE2 or L-SIGN. Cells were incubated at 37°C for an additional 1.5 days and were stained for β-galactosidase activity as described above.

Neutralizing mouse monoclonal antibodies (MAbs) against SARS-CoV S protein (44) were generously provided by Lia M. Haynes at the Centers for Disease Control and Prevention. Polyclonal mouse anti-SARS-CoV S-protein antiserum (22) was kindly provided by Chul-Joong Kim at Chung Nam National University, South Korea. Pseudoviruses were incubated with antibodies for 1 h at 37°C. Subsequently, the antibody-virus mixture was added to HeLa cells transfected with either ACE2 or L-SIGN. Cells were incubated at 37°C for 1.5 days and stained for β-galactosidase activity. Assays were done in duplicate.

To evaluate effects of endoglycosidase H (Endo H; New England Biolabs) on SARS-CoV pseudovirus infectivity, about 100 infectious units were treated with 500 U of enzyme for various times (0 to 4 h) in a nondenaturing condition. For controls, pseudoviruses were incubated with either normal culture medium or buffer only (50 mM sodium citrate, pH 5.5).

Western blotting. Freshly seeded TELCeB6 cells (less than 1 day old) were transfected as previously described (12, 13) with plasmids encoding either the wild-type (pHCMV-S) or mutant (pHCMV-S-μ) S gene using Lipofectin (Invitrogen). Three days posttransfection, culture medium was used as a source of SARS pseudovirus, and cells were lysed with a hypotonic buffer containing nonionic detergent (10 mM Tris, pH 7.5, 10 mM NaCl, 1.5 mM $MgCl_2$, and 1% NP-40) for protein analysis. Nuclei were removed by brief centrifugation. Postnuclear cell extracts were subjected to sodium dodecyl sulfate-polyacrylamide gel electrophoresis followed by electrotransfer to nitrocellulose membranes for Western blot analyses. SARS S proteins were detected with rabbit anti-S polyclonal antibodies (1:200 dilution of serum; generously provided by Shan Lu) (45) followed by goat anti-rabbit immunoglobulin G conjugated with horseradish peroxidase (Pierce). Protein bands were visualized with SuperSignal chemiluminescent substrates (Pierce) according to the manufacturer's protocol.

RESULTS

DC-SIGN and L-SIGN both serve as alternative receptors for SARS-CoV entry independently of ACE2. To determine whether DC-SIGN or L-SIGN could serve as alternative receptors for SARS-CoV rather than simply as enhancer factors, infectivity of SARS pseudoviruses (murine leukemia virus pseudotyped with S glycoprotein) was examined by using HeLa cells transfected with plasmids encoding these proteins. As shown in Fig. 1A, HeLa cells transfected with pcDNA empty vector were completely refractory to SARS pseudovirus infection. In contrast, cells transfected with ACE2-expressing plasmid efficiently supported pseudovirus infection. HeLa cells expressing either DC-SIGN or L-SIGN also were susceptible to infection, albeit considerably less so than those expressing ACE2. Although the difference was minimal and not statistically significant, cells expressing L-SIGN were consistently more susceptible to infection than those expressing DC-SIGN.

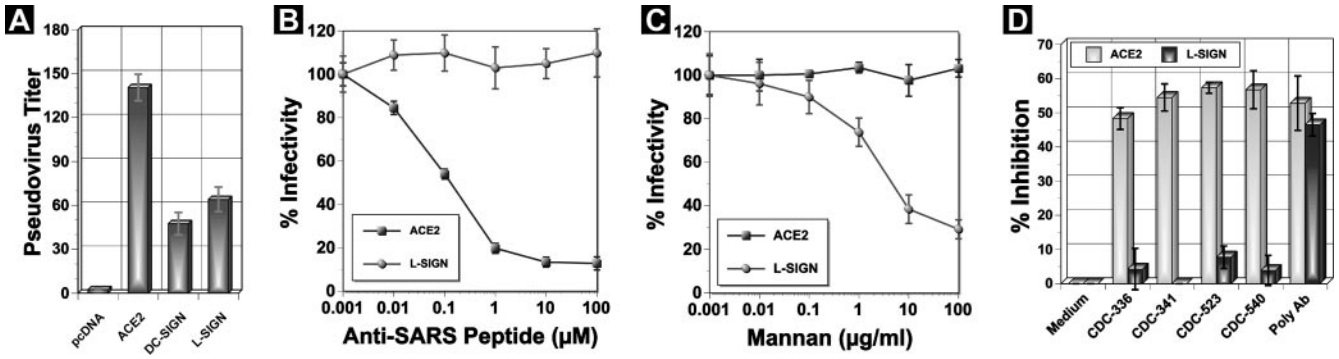

FIG. 1. DC-SIGN and L-SIGN serve as alternative receptors. (A) HeLa cells transfected with plasmids expressing ACE2, DC-SIGN, or L-SIGN were infected with SARS pseudoviruses. An empty vector (pcDNA) was used as a negative control. (B) ACE2- and L-SIGN-mediated infections were examined in the presence of various concentrations of an inhibitory peptide (P6) derived from ACE2 (13). (C) L-SIGN-mediated, but not ACE2-mediated, infections are inhibited by mannan in a dose-dependent manner. (D) Specific inhibition of ACE2-mediated infections by MAbs. A polyclonal anti-S-protein antiserum (poly Ab) from mice is able to inhibit infections mediated by both ACE2 and L-SIGN.

We have previously described the development of an ACE2-derived peptide (P6) that potently inhibits SARS pseudovirus infections of Vero E6 or HeLa cells expressing ACE2 with a 50% inhibitory concentration of approximately 100 nM (13). This peptide consists of two discontinuous segments of ACE2 (amino acid residues 22 to 44 and 351 to 357) artificially linked by a single glycine residue. These determinants have been shown to interact, biochemically and structurally, with the RBM of S protein and are critical for mediating SARS-CoV infection (23, 25). To unequivocally demonstrate that pseudovirus infections of HeLa cells expressing L-SIGN are not mediated through ACE2, infectivity was examined in the presence of the P6 peptide. As shown in Fig. 1B, infection mediated by ACE2 was potently inhibited by P6 peptide in a dose-dependent manner as previously described (13). In contrast, no inhibition was observed for L-SIGN-mediated infection, even in the presence of 100 μM. Similar results were observed for DC-SIGN-mediated infections (data not shown). These results not only indicate that DC/L-SIGN serve as alternative receptors but also indicate that the binding site(s) of these proteins on S protein is distinct from the site that ACE2 binds.

DC/L-SIGN are members of a C-type lectin family, the interactions of which with ligands are carbohydrate dependent (2, 14, 26); they specifically recognize high-mannose glycans (10). Mannan, a carbohydrate composed of high mannose, inhibits binding of ligands to DC/L-SIGN. To demonstrate that infections of HeLa cells expressing DC/L-SIGN by our SARS pseudoviruses are indeed mediated by DC/L-SIGN, infection of HeLa cells expressing either ACE2 or L-SIGN were carried out in the presence of various amounts of mannan (Fig. 1C). As expected, L-SIGN-mediated infections were inhibited by mannan in a dose-dependent manner. In contrast, ACE2-mediated infections were not affected by mannan.

To further characterize virus entry mediated by ACE2 and DC/L-SIGN, sensitivity of pseudoviruses to neutralizing MAbs was evaluated. Four MAbs (CDC-336, CDC-341, CDC-523, and CDC-540; obtained from Lia Haynes at the Centers for Disease Control and Prevention) were evaluated. These antibodies were generated from mice immunized with whole inactivated SARS-CoV particles (44). The epitope recognized by CDC-341 is amino acid residues 490 to 510, which is at the C-terminal end of the RBD. The epitopes of the other MAbs have not yet been determined. Regardless, all four MAbs inhibited ACE2-mediated virus entry (Fig. 1D). This is not surprising, since they were screened for their ability to block virus infection of Vero E6 cells. In contrast, none of the MAbs inhibited L-SIGN-mediated virus entry. This is not because L-SIGN-mediated infections are intrinsically difficult to inhibit, since polyclonal antiserum from mice immunized with *Lactobacillus casei* expressing S-protein fragments (22) was able to inhibit infections mediated by both receptors. Together, these results demonstrate that DC/L-SIGN can mediate SARS-CoV infections independently of ACE2.

DC/L-SIGN minimally enhance ACE2-mediated infections. Although the results of our study indicated that DC/L-SIGN function as alternative receptors for SARS-CoV, there remained a possibility that they also enhance ACE2-mediated infections. To evaluate whether there is a synergistic relationship between ACE2 and DC-SIGN or L-SIGN, pseudovirus infectivity in HeLa cells expressing various amounts of the latter proteins in the presence or the absence of ACE2 was evaluated. As expected, transfection of greater amounts of plasmid expressing DC-SIGN (Fig. 2A) or L-SIGN (Fig. 2B) increased pseudovirus infectivity. However, infectivity reached a plateau at about 0.5 μg of plasmid DNA, similar to what was observed with ACE2 (13). Consistent with results shown in Fig. 1A, L-SIGN was more efficient than DC-SIGN in supporting SARS pseudovirus entry. When ACE2-expressing plasmid was cotransfected (0.25 μg), a low level of synergy was observed. The maximal synergistic effect (1.6-fold over the additive level) was observed when 0.25 μg of plasmids expressing DC-SIGN or L-SIGN was used. The synergy was lost when 1 μg of plasmid was used. This is likely due to the fact that as DC/L-SIGN concentrations increase, they are removing a pool of viruses that can bind ACE2, rendering the virus infection less efficient. These results indicated that infections mediated by ACE2 and DC/L-SIGN are minimally synergistic and that the receptors likely function independently.

Glycans play an important role in SARS-CoV infections mediated by DC/L-SIGN. Since mannan inhibited SARS pseudovirus infections mediated by L-SIGN, glycans on S gly-

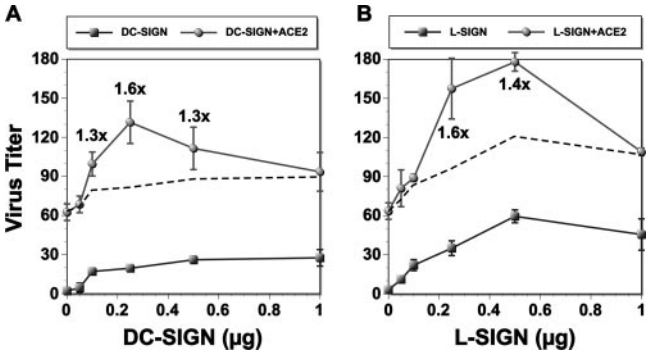

FIG. 2. Minimal synergy between ACE2 and DC/L-SIGN in SARS infection. SARS pseudovirus infections were carried out in HeLa cells transfected with various amounts of plasmids expressing DC-SIGN (A) or L-SIGN (B) with or without ACE2 (0.25 μg). A total of 1.25 μg of DNA was used, with pcDNA plasmid as a filler DNA. Dashed lines represent additive levels of infection.

coprotein most likely play an important role. To demonstrate this more directly, effects of removing carbohydrate moieties on pseudovirus infectivity were examined. We have previously shown that carbohydrate moieties on S protein are high-mannose and/or hybrid oligosaccharides and that they can be removed using Endo H under a mild condition (12). To remove glycans on S protein, pseudoviruses were treated with Endo H for different durations, from 0 to 4 h. Their infectivity was examined in HeLa cells expressing DC-SIGN, L-SIGN, or ACE2 (Fig. 3). As expected, infectivity of SARS pseudoviruses treated with Endo H decreased drastically in cells expressing DC-SIGN or L-SIGN in a time-dependent manner (Fig. 3A and B, respectively). In contrast, no reduction was observed for pseudoviruses incubated in either cell culture medium or buffer only. Not surprisingly, Endo H-treated pseudoviruses also lost infectivity in cells expressing ACE2, although the effect was significantly less pronounced than that for DC/L-SIGN-mediated infections; while it only took 30 or 50 min of Endo H treatment to observe 50% reduction in infectivity for DC-SIGN or L-SIGN, respectively, it took about 150 min for ACE2. Moreover, the maximal reduction in infectivity was less for ACE2 (approximately 60% for ACE2 and 80 and 70% for DC-SIGN and L-SIGN, respectively). Taken together, these results suggest that glycans are involved not only in binding DC/L-SIGN but also in maintaining the proper conformation of the protein required for efficient interaction with ACE2.

Glycans on specific sites are critical for L-SIGN-mediated infections. Treatment of glycoproteins with glycosidase allows only gross assessment of the potential importance of carbohydrate moieties in protein function, because glycans are removed indiscriminately. In addition, the removal of a large mass of glycans could alter global conformation of the protein structure. In this regard, characterizing S proteins with individual glycosylation sites eliminated by site-directed mutagenesis could provide more accurate information on the functional importance of glycans in virus entry. In particular, we were interested in (i) whether glycans at certain glycosylation sites are more important than others for virus entry and (ii) whether glycans at different sites have different roles in ACE2- and DC/L-SIGN-mediated infections.

There are 23 potential asparagine (N)-linked glycosylation sites on S protein (Fig. 4A). On a linear map of S glycoprotein, these sites appear to be distributed into three distinct clusters: cluster I at the N terminus (aa 29, 65, 73, 109, 118, 119, 158, 227, 269, 318, 330, and 357), cluster II in the middle of the protein near the border between S1- and S2-like domains (aa 589, 602, 691, 699, and 783), and cluster III at the C terminus (aa 1056, 1080, 1116, 1140, 1155, and 1176). To date, glycosylation at 13 of these sites (aa 118, 119, 227, 269, 318, 330, 357, 783, 1056, 1080, 1140, 1155, and 1176) have been confirmed by either mass spectrometric (19, 49) or biochemical (6) analyses. The glycosylation status of other sites needs to be further determined.

Since the S1 domain (aa 1 to ~680) (27, 41) is responsible for binding ACE2, we focused on characterizing 12 N-linked glycosylation sites in cluster I. Asparagine residues of the canonical NXS/T motif were individually mutated to glutamine (Q), which differs by only a single methylene group and represents the most conservative amino acid substitution. Twelve mutant SARS pseudoviruses were generated, and their infectivity in ACE2- or L-SIGN-expressing HeLa cells was compared to that of the wild-type pseudovirus. As shown in Fig.

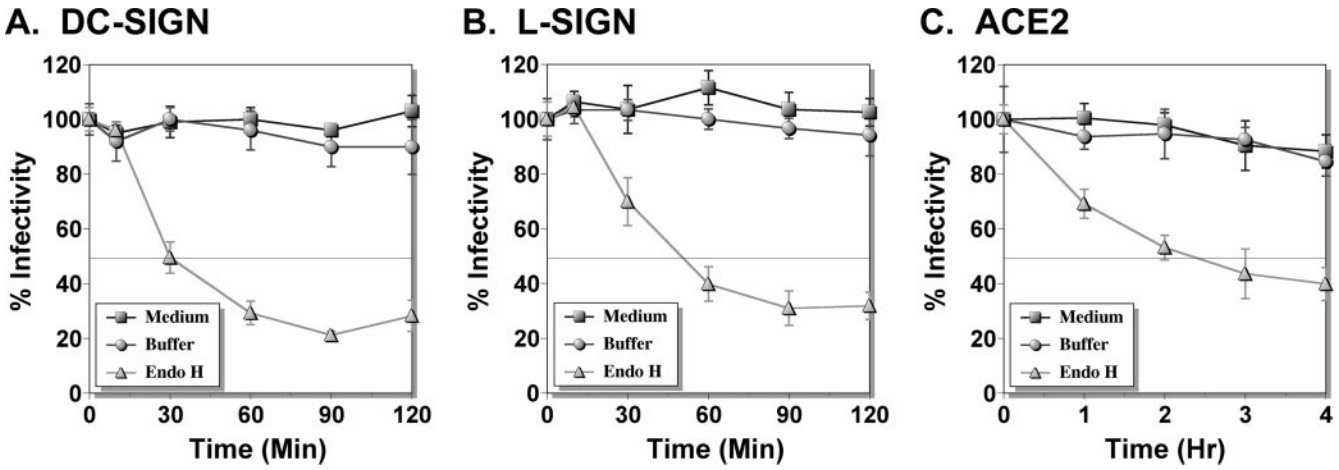

FIG. 3. Effects of deglycosylation on SARS-CoV infectivity. SARS pseudoviruses were treated with Endo H, buffer, or culture medium for various times, as indicated, at 37°C. Pseudoviruses subsequently were added to HeLa cells expressing DC-SIGN (A), L-SIGN (B), or ACE2 (C).

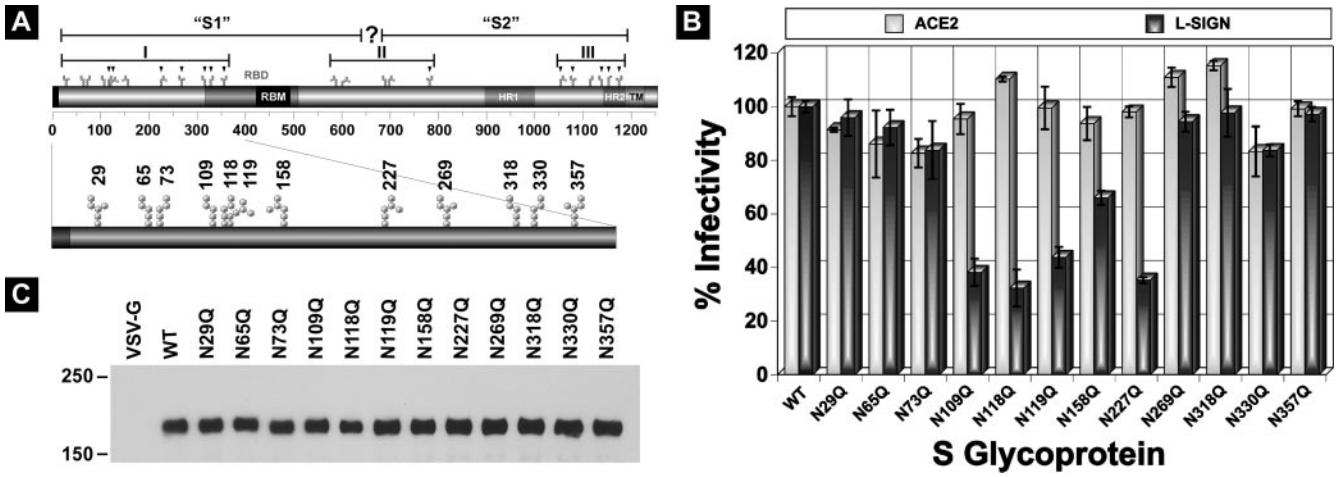

FIG. 4. Importance of specific glycosylation sites within cluster I for infections mediated by L-SIGN. (A) A schematic diagram of S glycoprotein and three clusters of potential N-linked glycosylation sites. Functional S1 and S2 domains, RBD and RBM, heptad repeat regions HR1 and HR2, and the transmembrane domain (TM) are indicated. Thirteen glycosylation sites, utilization of which was verified by mass spectrometry or biochemical analyses, are indicated by inverted triangles. (B) Effects of individual glycosylation site mutations on ACE2- or DC-SIGN-mediated SARS pseudovirus infectivity. (C) Western blot analyses of S-protein expression in TELCeB6 cells.

4B, all of the mutant pseudoviruses exhibited near-wild-type levels of infectivity in ACE2-expressing cells. In contrast, four mutants exhibited marked defects in their ability to use L-SIGN (mutants N109Q, N118Q, N119Q, and N227Q). Their infectivity was only about 30 to 40% of that of the wild-type pseudovirus. This reduction is significant, considering that the infectivity of pseudoviruses treated with Endo H was approximately 30% of that of the untreated virus (Fig. 3B). A modest, but reproducible, reduction in infectivity also was observed for mutant N158Q. The loss of infectivity by these five mutant pseudoviruses is most likely due to a reduced ability of mutant S proteins to specifically interact with L-SIGN rather than gross misfolding of the protein, since ACE2-mediated virus infection is virtually unaffected. Not surprisingly, all of the mutant S proteins were expressed normally as demonstrated by Western immunoblotting (Fig. 4C).

To further characterize five mutant S proteins, kinetic parameters of pseudovirus infectivity were evaluated. To do so, pseudovirus infectivity was reevaluated using a 20-min adsorption period (the time viruses are allowed to adsorb onto cells before the inoculum is removed) in addition to the typical 60 min. This was done because we have previously shown that ACE2-mediated infectivity begins to plateau by 60 min and that phenotypic differences between the wild-type and mutant ACE2 proteins were better observed using a 20-min period (13). The wild type and two mutants that did not exhibit significant defects (N29Q and N269Q) were examined as controls. As shown in Fig. 5A, the infectivity level of the wild-type pseudovirus at 20 min was about 70% of that at 60 min. The N29Q mutant pseudovirus exhibited an almost identical pattern. Although the level of infectivity of the N269Q mutant was slightly lower at 20 min, it increased to the wild-type level by 60 min. In contrast, the infectivity of the five other mutants was significantly lower than that of the wild type at 60 min. Interestingly, the infectivity of these mutants at 60 min was virtually identical to that at 20 min.

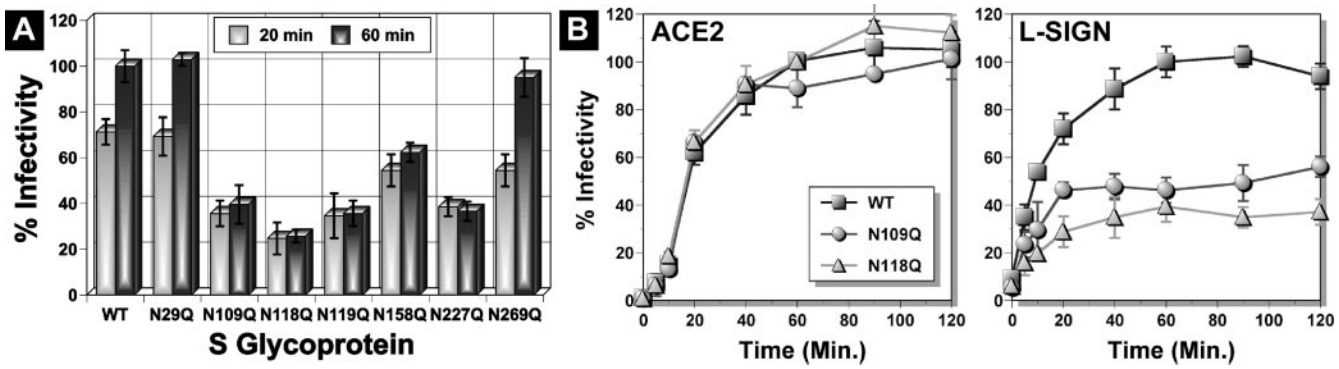

FIG. 5. Infection kinetic analyses of glycosylation site mutants. (A) HeLa cells expressing L-SIGN were infected with either wild-type (WT) or mutant SARS pseudoviruses. Pseudoviruses were adsorbed to cells for either 20 or 60 min before removing the inoculum. (B) Detailed infection kinetics for mutant pseudoviruses N109Q and N118Q in HeLa cells expressing either ACE2 or L-SIGN compared to those of the wild type. Pseudoviruses were adsorbed to cells for 0, 5, 10, 20, 40, 60, 90, or 120 min before removing inoculum. Data were normalized to the wild-type virus titer from the 60-min adsorption period.

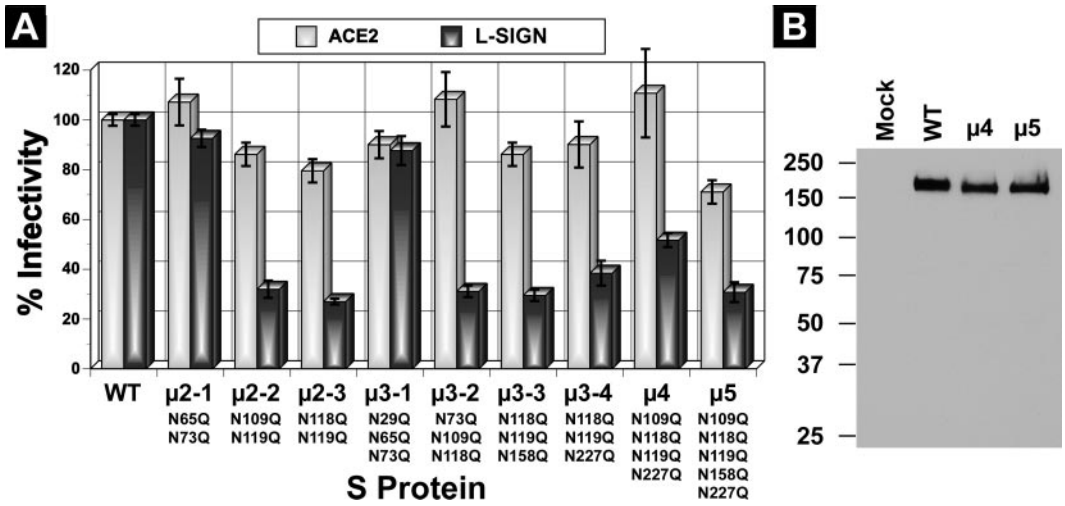

FIG. 6. Infectivity of multiple glycosylation site mutants. (A) HeLa cells expressing ACE2 or L-SIGN were infected with wild-type (WT) or mutant pseudoviruses. (B) Western blot analyses of mutant μ5 S-protein expression in TELCeB6 cells compared to that of the wild type or mutant μ4, which exhibited normal infectivity using ACE2.

To better understand this unexpected observation, more detailed ACE2- and L-SIGN-mediated infection kinetic analyses were performed for mutants N109Q and N118Q. As shown in Fig. 5B (left panel), both mutants exhibited infection kinetics similar to those of the wild type when ACE2 was used. However, when L-SIGN was used, the mutants exhibited markedly different kinetics (Fig. 5B, right panel). In contrast to the wild type, the infectivity of which continued to increase beyond 20 min, infectivity levels of mutant viruses reached a plateau in 20 min, consistent with the results shown in Fig. 5A. The precise reason for this observation is not yet clear. It is also interesting that the initial kinetic of infection mediated by L-SIGN appeared faster than that mediated by ACE2. While infectivity of the wild-type pseudovirus reached 35% using L-SIGN within 5 min of incubation, ACE2-mediated infection reached only about 5%. This suggests that interactions between L-SIGN and glycans are less specific, and therefore take less time, than those between ACE2 and the RBD of S protein.

Thus far, the results of our study demonstrated that glycans are important for DC/L-SIGN-mediated SARS-CoV entry and that 5 of 12 glycosylation sites in cluster I are critical (i.e., N109, N118, N119, N158, and N227). Although mutating each of these glycosylation sites resulted in substantial reduction in L-SIGN-mediated infectivity, none of them was completely disruptive. One likely explanation for this observation is that utilization of L-SIGN per se does not require the presence of all five glycosylation sites. However, efficient utilization may require a critical density of glycans and needs all five sites. Thus, eliminating any one of these sites would result in a reduction, but not complete loss, of infectivity.

We next asked whether efficiency in utilizing L-SIGN correlated with the available number of glycosylation sites. One could hypothesize that eliminating a greater number of glycosylation sites simultaneously would render the protein progressively less efficient in utilizing L-SIGN. To test this hypothesis, we generated nine additional S proteins with multiple mutations in various combinations (double, triple, quadruple, or pentuple) and evaluated the infectivity of pseudoviruses using ACE2 or L-SIGN. Not unexpectedly, combining N29Q, N65Q, and N73Q mutations (i.e., mutant μ2-1 or μ3-1), none of which affected virus infectivity individually, reduced neither ACE2- nor L-SIGN-mediated infectivity (Fig. 6A). In contrast, we were surprised to observe that combining individual mutations that reduced virus infectivity (i.e., N109Q, N118Q, N119Q, N158Q, and N227Q) did not significantly worsen the effect, even when all five sites were mutated simultaneously (i.e., mutant μ5). None of these mutants exhibited significant reduction in infectivity using ACE2, except for that of μ5, which was at about 70% of the wild-type level. The expression level of μ5 mutant S protein was not significantly different from that of μ4 or the wild-type proteins (Fig. 6B), suggesting that this reduction in ACE2-mediated infectivity is not due to a defect in protein expression. Instead, mutating five glycosylation sites all at once most likely partially altered the conformation of the ACE2-binding domain.

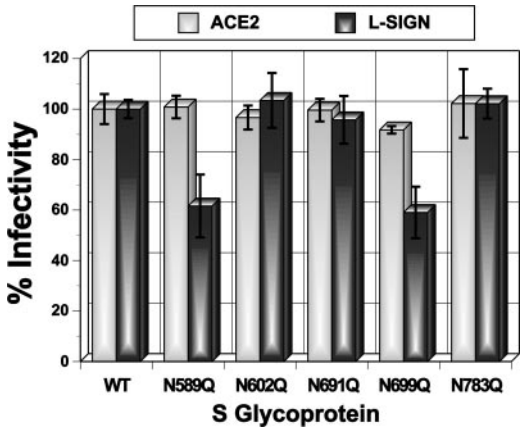

FIG. 7. Importance of specific glycosylation sites within cluster II for infections mediated by L-SIGN. HeLa cells expressing ACE2 or L-SIGN were infected with wild-type (WT) or mutant SARS pseudoviruses.

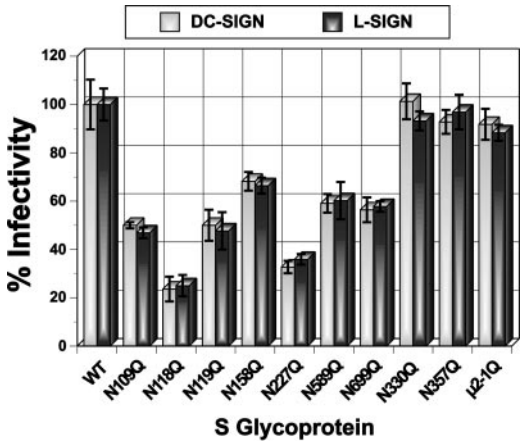

FIG. 8. N-linked glycosylation site mutants of SARS-CoV S protein affect both DC-SIGN and L-SIGN usage similarly. HeLa cells expressing DC-SIGN or L-SIGN were infected with wild-type (WT) or mutant SARS pseudoviruses. Mutant pseudovirus infectivity was normalized to that of the wild-type virus.

Incomplete loss of infectivity by the μ5 mutant could be explained if glycosylation sites outside of cluster I also could be utilized for DC/L-SIGN-mediated virus entry (Fig. 4A). The obvious alternative sites could be those within cluster II. To evaluate the potential role of glycosylation sites in cluster II, five additional mutant S proteins were generated (Fig. 7). Only two of the five proteins (N589Q and N699Q) exhibited partial loss (about 60% of the wild-type level) in L-SIGN-mediated infectivity. All of the mutants exhibited normal infectivity using ACE2 as a receptor. These results indicate that specific glycosylation sites in both clusters I and II play a role in DC/L-SIGN-mediated virus infections.

Despite seemingly less efficient utilization of DC-SIGN by SARS-CoV pseudoviruses compared to that of L-SIGN, we nonetheless examined the effects of N-linked glycosylation site mutations on DC-SIGN-mediated pseudovirus infectivity. All seven glycosylation site mutations that affected L-SIGN usage were evaluated (i.e., N109Q, N118Q, N119Q, N158Q, N227Q, N589Q, and N699Q). As shown in Fig. 8, DC-SIGN-mediated infections were affected in a manner similar to that of L-SIGN-mediated infections. As expected, no significant loss of infectivity was observed for N330Q, N357Q, or the μ2-1 double mutant (N65Q/N73Q). These results suggest that DC-SIGN- and L-SIGN-mediated infections likely proceed by a similar mechanism.

DISCUSSION

To date, the precise role of DC/L-SIGN in SARS-CoV infections is unclear and controversial. In a number of studies, DC/L-SIGN have been reported to function as infection enhancer factors but not as receptors (30, 39, 48); while these lectins capture and transfer viruses to neighboring target cells expressing ACE2, thereby facilitating infections in *trans*, they themselves did not appear to support virus infections directly. In contrast to these reports, Jeffers et al. (18) have shown that L-SIGN could serve as an alternative receptor. In agreement with the latter study, the results of our study clearly demonstrated that both DC-SIGN and L-SIGN do indeed serve as receptors independently of ACE2, albeit less efficiently (Fig. 1). The reason for the discrepancy is presently unknown.

One possible reason for the contradictory results is that different studies used different cell lines. While Jeffers et al. used CHO cells and we used HeLa cells, other studies used either quail-derived QT6 cells or B-THP-1 Raji B cells. If this speculation is true, then it raises the possibility that SARS-CoV uses a coreceptor, which could be present on CHO or HeLa cells but not on QT6 or B-THP-1 cells. Alternatively, DC/L-SIGN could be posttranslationally modified differently in different cell types, allowing the proteins on some cells to mediate virus infection but not those on others. Another possibility is that there could be subtle differences in membrane fluidity, which could affect the movement of membrane proteins within the lipid bilayer or membrane protein trafficking among different cell types. Regardless, additional studies will be necessary to better define the functional properties of DC/L-SIGN in SARS-CoV infections.

In this study, we have identified seven potential N-linked glycosylation sites that play an important role in L-SIGN-mediated SARS-CoV entry. They include residues N109, N118, N119, N158, and N227 within cluster I and N589 and N699 within cluster II. It should be mentioned that, to date, glycosylation has been positively confirmed physicochemically only for residues N118, N119, and N227 (6, 19, 49) (Fig. 4A). However, asparagine residues at N109, N158, N589, and N699 are most likely glycosylated on the basis of the facts that (i) mutating these sites specifically diminished L-SIGN-mediated infections but not those mediated by ACE2, and (ii) mutating 10 other asparagine residues did not nonspecifically affect virus infectivity. Regardless of whether these asparagine residues are actually glycosylated or not, the results of our study indicate that these amino acids are critical for L-SIGN-mediated virus infections.

It is interesting that two glycosylation sites in cluster II are located distant from the five sites in cluster I (Fig. 9A). This result raises a question as to whether the glycosylation sites in the two clusters are indeed physically separated or whether they actually lie close together on a tertiary structure of the protein. Solving a crystal structure of an intact protein will be needed to address this question. It also is noteworthy that all seven glycosylation sites are situated clearly outside of the ACE2-binding domain (aa 318 to 510). In this regard, it was somewhat surprising that four glycosylation sites located close to or within the ACE2-binding domain (N269, N318, N330, and N357) were dispensable for DC/L-SIGN-mediated infections. Although we can speculate (see below), we do not yet know why only certain glycosylation sites are capable of mediating infections through DC/L-SIGN.

In a recently reported study, it has been suggested that a region between amino acid residues 324 and 386 of S protein was the minimal DC-SIGN-binding domain and that glycosylation sites N330 and N357 are involved in DC-SIGN-mediated SARS-CoV infections (39). This conclusion was based on the following observations. First, a recombinant baculovirus that expressed amino acid residues 17 to 386 of S protein fused to a truncated baculovirus envelope glycoprotein, gp64, was able to bind B-THP-1 cells expressing DN-SIGN but not a virus that expressed residues 17 to 324. Second, an epitope

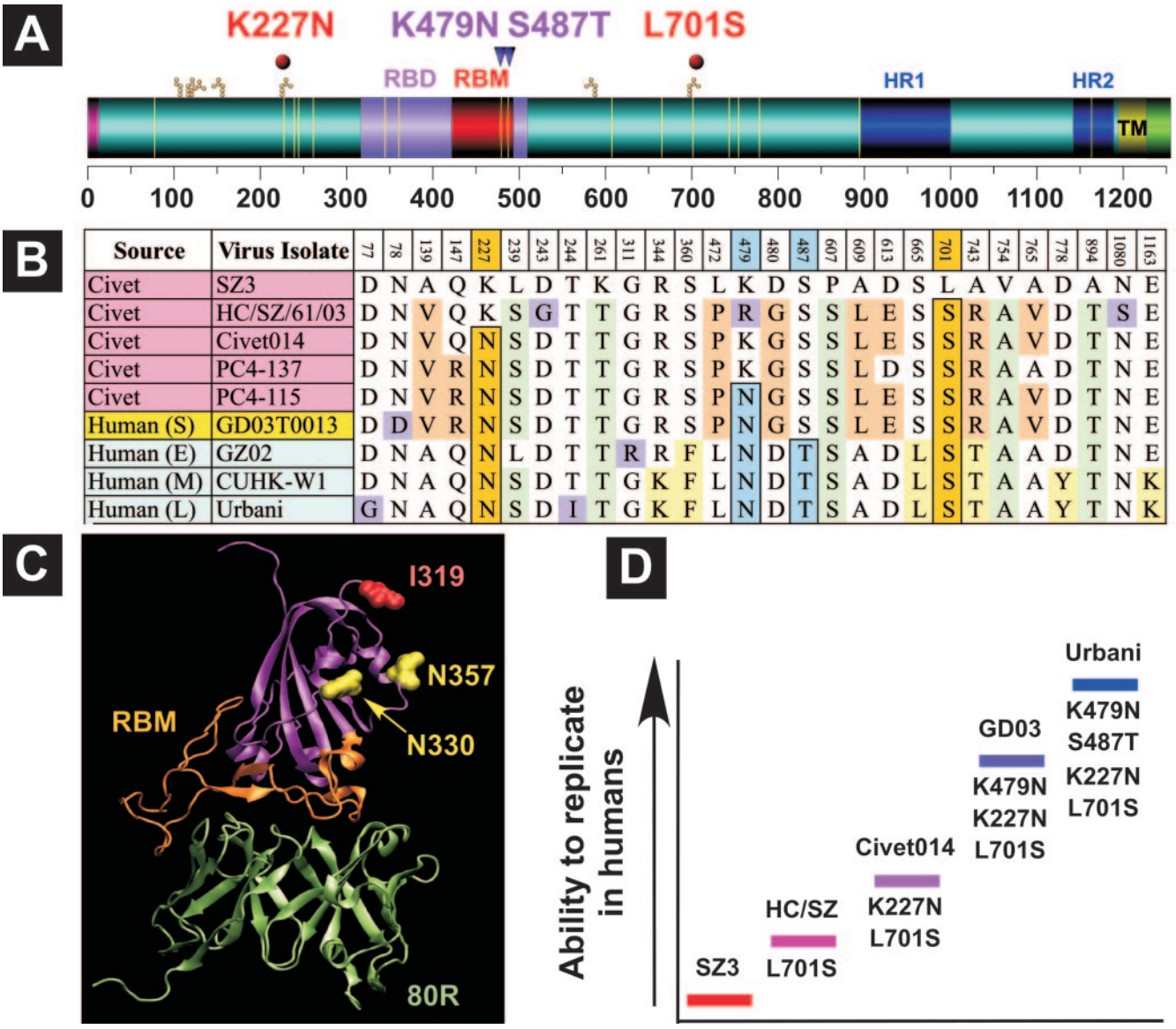

FIG. 9. Role of N-linked glycosylation sites in S-protein function. (A) A schematic diagram of S glycoprotein. Locations of seven glycosylation sites important for DC/L-SIGN-mediated infections are shown. Yellow lines indicate positions of 17 amino acids that are different between SZ3 and Urbani. Amino acid changes critical for efficient usage of human ACE2 (K479N and S487T) are identified by inverted triangles. Amino acid changes that introduced two novel N-linked glycosylation sites are shown with red dots (K227N and L701S). (B) Amino acid sequences of S proteins of viruses isolated from civets and humans. Viruses isolated from humans at different phases of the epidemic are indicated (S, sporadic; E, early; M, middle; and L, late). Amino acid sequences are compared to that of the SZ3 isolate, and they are color coded as follows: tan, changes found predominantly in civets; yellow, changes found mostly in human isolates; green, changes found both in human and civet isolates; light blue, changes critical for human ACE2 usage; orange, changes that introduce two novel glycosylation sites; and purple, sporadic changes. Numbers indicate amino acid positions. (C) A crystal structure of an RBD of S protein complexed with neutralizing antibody 80R (15) (Protein Data Bank file 2GHW). The RBM and locations of glycosylation sites N330 and N357 are shown. The first residue of the RBD (I319) shows the likely position of glycosylation site N318. The 2GHW file was used because it included residues closest to N318. (D) Likely ability of different SARS-CoV isolates to replicate in humans. Isolate names and critical amino acid changes that could have facilitated zoonotic transmission of the virus are indicated.

recognized by a monoclonal antibody that prevents binding of SARS-CoV to DC-SIGN was mapped to amino acid residues 363 to 368. Third, mutating N330 and/or N357 to glutamine partially reduced the infectivity of SARS-CoV pseudoviruses.

Despite seemingly contradictory results, it should be emphasized that the two studies are fundamentally different. In our study, we examined glycosylation sites that are critical for direct virus entry (i.e., using DC/L-SIGN only, independently of ACE2). In contrast, Shih et al. (39) examined glycosylation sites important for capturing viruses by DC-SIGN-expressing B-THP-1 cells and subsequent *trans*-infection of HepG2 target cells that express ACE2.

Besides the difference in the nature of the assay, we feel that Shih et al. (39) may have overlooked the importance of other glycosylation sites for the following reasons. First, expression of amino acid residues 17 to 324 fused to baculovirus gp64

could have resulted in a misfolded protein. Therefore, to conclude simply that glycosylation sites between amino acids 17 and 324 are not involved in binding DC-SIGN is somewhat flawed. Second, the glycosylation pattern of S glycoprotein expressed in insect cells could be significantly different from that expressed in mammalian cells, in terms of both site usage and types of modifications. In fact, our recent mass spectrometry analyses of S1 protein expressed in insect cells using a recombinant baculovirus (4) have shown that residues N227 and N269 are not glycosylated (unpublished data). Third, they utilized only a limited number of MAbs to identify ones that can block DC-SIGN-mediated *trans*-infection. Finally, Shih et al. (39) did not examine the effects of mutating other glycosylation sites.

According to our data, glycosylation sites at N330 and N357 do not support direct infections mediated by L-SIGN (Fig. 4B). However, these residues have been implicated in binding DC-SIGN and in mediating *trans*-infections (39). Together, these results seem to suggest that binding of DC/L-SIGN to glycans at these sites, unlike the seven sites we found to be important, does not lead to an eventual fusion of viral and cellular membranes. This failure could be due to certain geometrical constraints that prevent one of the post-receptor-binding events from occurring (e.g., conformational changes in S protein or insertion of a hydrophobic fusion domain into the cellular membrane). Examination of a crystal structure of the (ACE2) RBD shows that N330 and N357 are located distant from the RBM (Fig. 9C). N318, which also does not support direct infections mediated by DC/L-SIGN, is situated even further away (inferred based on the position of I319 on the crystal structure). These residues are located on a plane that is perpendicular to that of the RBM. One could speculate that such orientation prevents the protein from undergoing proper conformational changes. Determination of the structure of an intact protein (or at least the entire S1 domain) could facilitate better understanding of post-receptor-binding events of SARS-CoV entry processes.

Although the exact origin of SARS-CoV responsible for the 2002 and 2003 epidemic is unknown, molecular phylogenetic analyses and epidemiological studies indicate clear zoonotic transmission of the virus (11, 40). One likely source is Himalayan palm civets (*Paguma larvata*). Amino acid sequence analyses of S glycoproteins of viruses isolated from civets (SZ3) and humans (Urbani) revealed a difference of 17 residues (Fig. 9B). Two of these changes, which lie within the RBM (K479N and S487T), have been shown to be critical for efficient binding to human ACE2 (25, 36). Plotting the mutations on a linear diagram of S glycoprotein revealed two major clusters of mutations (227 to 261 and 607 to 778), which suggests the importance of some of these changes for adaptations to grow in human cells (Fig. 9A). Interestingly, we noticed that mutations K227N and L701S have introduced two novel N-linked glycosylation sites at N227 and N699, both of which we found were important for L-SIGN-mediated infections (Fig. 4B and 7).

Extensive database searches of SARS-CoV S glycoproteins showed that K227N and L701S mutations are found in all viruses isolated from humans. Among viruses isolated from civets, there were strains with the L701S mutation alone (e.g., HC/SZ/61/03) or both K227N and L701S mutations (e.g., Civet014 or PC4-137). These viruses contained neither K479N nor S487T mutation. Some viruses contained both K227N and L701S mutations as well as K479N (e.g., PC4-115 isolated from a civet and GD03T0013 isolated from a human patient). From these observations, together with the fact that SZ3 is extremely poor in infecting cells using human ACE2, it is tempting to speculate that the two glycosylation sites at N227 and N699 have facilitated zoonotic transmission of SARS-CoV. As diagrammed in Fig. 9D, SZ3 virus infection in humans might not be productive due to inefficient utilization of human ACE2 by the virus. However, a virus with glycosylation sites at N227 and/or N699 could replicate in humans better than SZ3 using DC/L-SIGN. This could provide opportunities for producing variants with K479N and/or S487T mutations, allowing the mutant viruses to efficiently utilize human ACE2. More detailed phylogenetic analyses using a greater number of virus isolates and additional site-directed mutagenesis studies will be required to provide conclusive answers.

ACKNOWLEDGMENTS

We are grateful to François-Loïc Cosset, Michael Farzan, Lia Haynes, Shan Lu, and Chul-Joong Kim for sharing valuable reagents. The following reagents were obtained through the AIDS Research and Reference Reagent Program, NIAID, NIH: pcDNA-3-DC-SIGN from S. Pöhlmann, F. Baribaud, F. Kirchhoff, and R. W. Doms; and pcDNA3-DC-SIGNR from Stefan Pöhlmann, Elizabeth Soilleux, Frédéric Baribaud, and Robert W. Doms.

This work was supported by NIH grant U54 AI057160 to the Midwest Regional Center of Excellence for Biodefense and Emerging Infectious Diseases Research (MRCE) and by R21 AI059217.

REFERENCES

1. **Abraham, S., T. E. Kienzle, W. Lapps, and D. A. Brian.** 1990. Deduced sequence of the bovine coronavirus spike protein and identification of the internal proteolytic cleavage site. Virology **176:**296–301.
2. **Appelmelk, B. J., I. van Die, S. J. van Vliet, C. M. Vandenbroucke-Grauls, T. B. Geijtenbeek, and Y. van Kooyk.** 2003. Cutting edge: carbohydrate profiling identifies new pathogens that interact with dendritic cell-specific ICAM-3-grabbing nonintegrin on dendritic cells. J. Immunol. **170:**1635–1639.
3. **Babcock, G. J., D. J. Esshaki, W. D. Thomas, Jr., and D. M. Ambrosino.** 2004. Amino acids 270 to 510 of the severe acute respiratory syndrome coronavirus spike protein are required for interaction with receptor. J. Virol. **78:**4552–4560.
4. **Bisht, H., A. Roberts, L. Vogel, K. Subbarao, and B. Moss.** 2005. Neutralizing antibody and protective immunity to SARS coronavirus infection of mice induced by a soluble recombinant polypeptide containing an N-terminal segment of the spike glycoprotein. Virology **334:**160–165.
5. **Bosch, B. J., B. E. Martina, R. Van Der Zee, J. Lepault, B. J. Haijema, C. Versluis, A. J. Heck, R. De Groot, A. D. Osterhaus, and P. J. Rottier.** 2004. Severe acute respiratory syndrome coronavirus (SARS-CoV) infection inhibition using spike protein heptad repeat-derived peptides. Proc. Natl. Acad. Sci. USA **101:**8455–8460.
6. **Chakraborti, S., P. Prabakaran, X. Xiao, and D. S. Dimitrov.** 2005. The SARS coronavirus S glycoprotein receptor binding domain: fine mapping and functional characterization. Virol. J. **2:**73.
7. **Chan, V. S., K. Y. Chan, Y. Chen, L. L. Poon, A. N. Cheung, B. Zheng, K. H. Chan, W. Mak, H. Y. Ngan, X. Xu, G. Screaton, P. K. Tam, J. M. Austyn, L. C. Chan, S. P. Yip, M. Peiris, U. S. Khoo, and C. L. Lin.** 2006. Homozygous L-SIGN (CLEC4M) plays a protective role in SARS coronavirus infection. Nat. Genet. **38:**38–46.
8. **Chow, K. C., C. H. Hsiao, T. Y. Lin, C. L. Chen, and S. H. Chiou.** 2004. Detection of severe acute respiratory syndrome-associated coronavirus in pneumocytes of the lung. Am. J. Clin. Pathol. **121:**574–580.
9. **Drosten, C., S. Gunther, W. Preiser, S. van der Werf, H. R. Brodt, S. Becker, H. Rabenau, M. Panning, L. Kolesnikova, R. A. Fouchier, A. Berger, A. M. Burguiere, J. Cinatl, M. Eickmann, N. Escriou, K. Grywna, S. Kramme, J. C. Manuguerra, S. Muller, V. Rickerts, M. Sturmer, S. Vieth, H. D. Klenk, A. D. Osterhaus, H. Schmitz, and H. W. Doerr.** 2003. Identification of a novel coronavirus in patients with severe acute respiratory syndrome. N. Engl. J. Med. **348:**1967–1976.
10. **Feinberg, H., D. A. Mitchell, K. Drickamer, and W. I. Weis.** 2001. Structural basis for selective recognition of oligosaccharides by DC-SIGN and DC-SIGNR. Science **294:**2163–2166.

11. **Guan, Y., B. J. Zheng, Y. Q. He, X. L. Liu, Z. X. Zhuang, C. L. Cheung, S. W. Luo, P. H. Li, L. J. Zhang, Y. J. Guan, K. M. Butt, K. L. Wong, K. W. Chan, W. Lim, K. F. Shortridge, K. Y. Yuen, J. S. Peiris, and L. L. Poon.** 2003. Isolation and characterization of viruses related to the SARS coronavirus from animals in southern China. Science **302:**276–278.
12. **Han, D. P., H. G. Kim, Y. B. Kim, L. L. Poon, and M. W. Cho.** 2004. Development of a safe neutralization assay for SARS-CoV and characterization of S-glycoprotein. Virology **326:**140–149.
13. **Han, D. P., A. Penn-Nicholson, and M. W. Cho.** 2006. Identification of critical determinants on ACE2 for SARS-CoV entry and development of a potent entry inhibitor. Virology **350:**15–25.
14. **Hong, P. W., K. B. Flummerfelt, A. de Parseval, K. Gurney, J. H. Elder, and B. Lee.** 2002. Human immunodeficiency virus envelope (gp120) binding to DC-SIGN and primary dendritic cells is carbohydrate dependent but does not involve 2G12 or cyanovirin binding sites: implications for structural analyses of gp120-DC-SIGN binding. J. Virol. **76:**12855–12865.
15. **Hwang, W. C., Y. Lin, E. Santelli, J. Sui, L. Jaroszewski, B. Stec, M. Farzan, W. A. Marasco, and R. C. Liddington.** 2006. Structural basis of neutralization by a human anti-severe acute respiratory syndrome spike protein antibody, 80R. J. Biol. Chem. **281:**34610–34616.
16. **Ingallinella, P., E. Bianchi, M. Finotto, G. Cantoni, D. M. Eckert, V. M. Supekar, C. Bruckmann, A. Carfi, and A. Pessi.** 2004. Structural characterization of the fusion-active complex of severe acute respiratory syndrome (SARS) coronavirus. Proc. Natl. Acad. Sci. USA **101:**8709–8714.
17. **Jackwood, M. W., D. A. Hilt, S. A. Callison, C. W. Lee, H. Plaza, and E. Wade.** 2001. Spike glycoprotein cleavage recognition site analysis of infectious bronchitis virus. Avian Dis. **45:**366–372.
18. **Jeffers, S. A., S. M. Tusell, L. Gillim-Ross, E. M. Hemmila, J. E. Achenbach, G. J. Babcock, W. D. Thomas, Jr., L. B. Thackray, M. D. Young, R. J. Mason, D. M. Ambrosino, D. E. Wentworth, J. C. Demartini, and K. V. Holmes.** 2004. CD209L (L-SIGN) is a receptor for severe acute respiratory syndrome coronavirus. Proc. Natl. Acad. Sci. USA **101:**15748–15753.
19. **Krokhin, O., Y. Li, A. Andonov, H. Feldmann, R. Flick, S. Jones, U. Stroeher, N. Bastien, K. V. Dasuri, K. Cheng, J. N. Simonsen, H. Perreault, J. Wilkins, W. Ens, F. Plummer, and K. G. Standing.** 2003. Mass spectrometric characterization of proteins from the sars virus: a preliminary report. Mol. Cell. Proteomics **2:**346–356.
20. **Ksiazek, T. G., D. Erdman, C. S. Goldsmith, S. R. Zaki, T. Peret, S. Emery, S. Tong, C. Urbani, J. A. Comer, W. Lim, P. E. Rollin, S. F. Dowell, A. E. Ling, C. D. Humphrey, W. J. Shieh, J. Guarner, C. D. Paddock, P. Rota, B. Fields, J. DeRisi, J. Y. Yang, N. Cox, J. M. Hughes, J. W. LeDuc, W. J. Bellini, and L. J. Anderson.** 2003. A novel coronavirus associated with severe acute respiratory syndrome. N. Engl. J. Med. **348:**1953–1966.
21. **Lau, S. K., P. C. Woo, K. S. Li, Y. Huang, H. W. Tsoi, B. H. Wong, S. S. Wong, S. Y. Leung, K. H. Chan, and K. Y. Yuen.** 2005. Severe acute respiratory syndrome coronavirus-like virus in Chinese horseshoe bats. Proc. Natl. Acad. Sci. USA **102:**14040–14045.
22. **Lee, J. S., H. Poo, D. P. Han, S. P. Hong, K. Kim, M. W. Cho, E. Kim, M. H. Sung, and C. J. Kim.** 2006. Mucosal immunization with surface-displayed severe acute respiratory syndrome coronavirus spike protein on *Lactobacillus casei* induces neutralizing antibodies in mice. J. Virol. **80:**4079–4087.
23. **Li, F., W. Li, M. Farzan, and S. C. Harrison.** 2006. Interactions between SARS coronavirus and its receptor. Adv. Exp. Med. Biol. **581:**229–234.
24. **Li, W., M. J. Moore, N. Vasilieva, J. Sui, S. K. Wong, M. A. Berne, M. Somasundaran, J. L. Sullivan, K. Luzuriaga, T. C. Greenough, H. Choe, and M. Farzan.** 2003. Angiotensin-converting enzyme 2 is a functional receptor for the SARS coronavirus. Nature **426:**450–454.
25. **Li, W., C. Zhang, J. Sui, J. H. Kuhn, M. J. Moore, S. Luo, S. K. Wong, I. C. Huang, K. Xu, N. Vasilieva, A. Murakami, Y. He, W. A. Marasco, Y. Guan, H. Choe, and M. Farzan.** 2005. Receptor and viral determinants of SARS-coronavirus adaptation to human ACE2. EMBO J. **24:**1634–1643.
26. **Lin, G., G. Simmons, S. Pohlmann, F. Baribaud, H. Ni, G. J. Leslie, B. S. Haggarty, P. Bates, D. Weissman, J. A. Hoxie, and R. W. Doms.** 2003. Differential N-linked glycosylation of human immunodeficiency virus and Ebola virus envelope glycoproteins modulates interactions with DC-SIGN and DC-SIGNR. J. Virol. **77:**1337–1346.
27. **Liò, P., and N. Goldman.** 2004. Phylogenomics and bioinformatics of SARS-CoV. Trends Microbiol. **12:**106–111.
28. **Marra, M. A., S. J. Jones, C. R. Astell, R. A. Holt, A. Brooks-Wilson, Y. S. Butterfield, J. Khattra, J. K. Asano, S. A. Barber, S. Y. Chan, A. Cloutier, S. M. Coughlin, D. Freeman, N. Girn, O. L. Griffith, S. R. Leach, M. Mayo, H. McDonald, S. B. Montgomery, P. K. Pandoh, A. S. Petrescu, A. G. Robertson, J. E. Schein, A. Siddiqui, D. E. Smailus, J. M. Stott, G. S. Yang, F. Plummer, A. Andonov, H. Artsob, N. Bastien, K. Bernard, T. F. Booth, D. Bowness, M. Czub, M. Drebot, L. Fernando, R. Flick, M. Garbutt, M. Gray, A. Grolla, S. Jones, H. Feldmann, A. Meyers, A. Kabani, Y. Li, S. Normand, U. Stroher, G. A. Tipples, S. Tyler, R. Vogrig, D. Ward, B. Watson, R. C. Brunham, M. Krajden, M. Petric, D. M. Skowronski, C. Upton, and R. L. Roper.** 2003. The genome sequence of the SARS-associated coronavirus. Science **300:**1399–1404.
29. **Martina, B. E., B. L. Haagmans, T. Kuiken, R. A. Fouchier, G. F. Rimmelzwaan, G. Van Amerongen, J. S. Peiris, W. Lim, and A. D. Osterhaus.** 2003. Virology: SARS virus infection of cats and ferrets. Nature **425:**915.
30. **Marzi, A., T. Gramberg, G. Simmons, P. Moller, A. J. Rennekamp, M. Krumbiegel, M. Geier, J. Eisemann, N. Turza, B. Saunier, A. Steinkasserer, S. Becker, P. Bates, H. Hofmann, and S. Pohlmann.** 2004. DC-SIGN and DC-SIGNR interact with the glycoprotein of Marburg virus and the S protein of severe acute respiratory syndrome coronavirus. J. Virol. **78:**12090–12095.
31. **Mounir, S., and P. J. Talbot.** 1993. Molecular characterization of the S protein gene of human coronavirus OC43. J. Gen. Virol. **74:**1981–1987.
32. **Peiris, J. S., S. T. Lai, L. L. Poon, Y. Guan, L. Y. Yam, W. Lim, J. Nicholls, W. K. Yee, W. W. Yan, M. T. Cheung, V. C. Cheng, K. H. Chan, D. N. Tsang, R. W. Yung, T. K. Ng, and K. Y. Yuen.** 2003. Coronavirus as a possible cause of severe acute respiratory syndrome. Lancet **361:**1319–1325.
33. **Pöhlmann, S., F. Baribaud, B. Lee, G. J. Leslie, M. D. Sanchez, K. Hiebenthal-Millow, J. Munch, F. Kirchhoff, and R. W. Doms.** 2001. DC-SIGN interactions with human immunodeficiency virus type 1 and 2 and simian immunodeficiency virus. J. Virol. **75:**4664–4672.
34. **Pöhlmann, S., E. J. Soilleux, F. Baribaud, G. J. Leslie, L. S. Morris, J. Trowsdale, B. Lee, N. Coleman, and R. W. Doms.** 2001. DC-SIGNR, a DC-SIGN homologue expressed in endothelial cells, binds to human and simian immunodeficiency viruses and activates infection in trans. Proc. Natl. Acad. Sci. USA **98:**2670–2675. Pöhlma
35. **Poutanen, S. M., D. E. Low, B. Henry, S. Finkelstein, D. Rose, K. Green, R. Tellier, R. Draker, D. Adachi, M. Ayers, A. K. Chan, D. M. Skowronski, I. Salit, A. E. Simor, A. S. Slutsky, P. W. Doyle, M. Krajden, M. Petric, R. C. Brunham, and A. J. McGeer.** 2003. Identification of severe acute respiratory syndrome in Canada. N. Engl. J. Med. **348:**1995–2005.
36. **Qu, X. X., P. Hao, X. J. Song, S. M. Jiang, Y. X. Liu, P. G. Wang, X. Rao, H. D. Song, S. Y. Wang, Y. Zuo, A. H. Zheng, M. Luo, H. L. Wang, F. Deng, H. Z. Wang, Z. H. Hu, M. X. Ding, G. P. Zhao, and H. K. Deng.** 2005. Identification of two critical amino acid residues of the severe acute respiratory syndrome coronavirus spike protein for its variation in zoonotic tropism transition via a double substitution strategy. J. Biol. Chem. **280:**29588–29595.
37. **Rota, P. A., M. S. Oberste, S. S. Monroe, W. A. Nix, R. Campagnoli, J. P. Icenogle, S. Penaranda, B. Bankamp, K. Maher, M. H. Chen, S. Tong, A. Tamin, L. Lowe, M. Frace, J. L. DeRisi, Q. Chen, D. Wang, D. D. Erdman, T. C. Peret, C. Burns, T. G. Ksiazek, P. E. Rollin, A. Sanchez, S. Liffick, B. Holloway, J. Limor, K. McCaustland, M. Olsen-Rasmussen, R. Fouchier, S. Gunther, A. D. Osterhaus, C. Drosten, M. A. Pallansch, L. J. Anderson, and W. J. Bellini.** 2003. Characterization of a novel coronavirus associated with severe acute respiratory syndrome. Science **300:**1394–1399.
38. **Schnierle, B. S., J. Stitz, V. Bosch, F. Nocken, H. Merget-Millitzer, M. Engelstadter, R. Kurth, B. Groner, and K. Cichutek.** 1997. Pseudotyping of murine leukemia virus with the envelope glycoproteins of HIV generates a retroviral vector with specificity of infection for CD4-expressing cells. Proc. Natl. Acad. Sci. USA **94:**8640–8645.
39. **Shih, Y. P., C. Y. Chen, S. J. Liu, K. H. Chen, Y. M. Lee, Y. C. Chao, and Y. M. Chen.** 2006. Identifying epitopes responsible for neutralizing antibody and DC-SIGN binding on the spike glycoprotein of the severe acute respiratory syndrome coronavirus. J. Virol. **80:**10315–10324.
40. **Song, H. D., C. C. Tu, G. W. Zhang, S. Y. Wang, K. Zheng, L. C. Lei, Q. X. Chen, Y. W. Gao, H. Q. Zhou, H. Xiang, H. J. Zheng, S. W. Chern, F. Cheng, C. M. Pan, H. Xuan, S. J. Chen, H. M. Luo, D. H. Zhou, Y. F. Liu, J. F. He, P. Z. Qin, L. H. Li, Y. Q. Ren, W. J. Liang, Y. D. Yu, L. Anderson, M. Wang, R. H. Xu, X. W. Wu, H. Y. Zheng, J. D. Chen, G. Liang, Y. Gao, M. Liao, L. Fang, L. Y. Jiang, H. Li, F. Chen, B. Di, L. J. He, J. Y. Lin, S. Tong, X. Kong, L. Du, P. Hao, H. Tang, A. Bernini, X. J. Yu, O. Spiga, Z. M. Guo, H. Y. Pan, W. Z. He, J. C. Manuguerra, A. Fontanet, A. Danchin, N. Niccolai, Y. X. Li, C. I. Wu, and G. P. Zhao.** 2005. Cross-host evolution of severe acute respiratory syndrome coronavirus in palm civet and human. Proc. Natl. Acad. Sci. USA **102:**2430–2435.
41. **Spiga, O., A. Bernini, A. Ciutti, S. Chiellini, N. Menciassi, F. Finetti, V. Causarono, F. Anselmi, F. Prischi, and N. Niccolai.** 2003. Molecular modelling of S1 and S2 subunits of SARS coronavirus spike glycoprotein. Biochem. Biophys. Res. Commun. **310:**78–83.
42. **To, K. F., and A. W. Lo.** 2004. Exploring the pathogenesis of severe acute respiratory syndrome (SARS): the tissue distribution of the coronavirus (SARS-CoV) and its putative receptor, angiotensin-converting enzyme 2 (ACE2). J. Pathol. **203:**740–743.
43. **Tripet, B., M. W. Howard, M. Jobling, R. K. Holmes, K. V. Holmes, and R. S. Hodges.** 2004. Structural characterization of the SARS-coronavirus spike S fusion protein core. J. Biol. Chem. **279:**20836–20849.
44. **Tripp, R. A., L. M. Haynes, D. Moore, B. Anderson, A. Tamin, B. H. Harcourt, L. P. Jones, M. Yilla, G. J. Babcock, T. Greenough, D. M. Ambrosino, R. Alvarez, J. Callaway, S. Cavitt, K. Kamrud, H. Alterson, J. Smith, J. L. Harcourt, C. Miao, R. Razdan, J. A. Comer, P. E. Rollin, T. G. Ksiazek, A. Sanchez, P. A. Rota, W. J. Bellini, and L. J. Anderson.** 2005. Monoclonal antibodies to SARS-associated coronavirus (SARS-CoV): identification of neutralizing and antibodies reactive to S, N, M and E viral proteins. J. Virol. Methods **128:**21–28.

45. **Wang, S., T. H. Chou, P. V. Sakhatskyy, S. Huang, J. M. Lawrence, H. Cao, X. Huang, and S. Lu.** 2005. Identification of two neutralizing regions on the severe acute respiratory syndrome coronavirus spike glycoprotein produced from the mammalian expression system. J. Virol. **79:**1906–1910.
46. **Wong, S. K., W. Li, M. J. Moore, H. Choe, and M. Farzan.** 2004. A 193-amino acid fragment of the SARS coronavirus S protein efficiently binds angiotensin-converting enzyme 2. J. Biol. Chem. **279:**3197–3201.
47. **Xiao, X., S. Chakraborti, A. S. Dimitrov, K. Gramatikoff, and D. S. Dimitrov.** 2003. The SARS-CoV S glycoprotein: expression and functional characterization. Biochem. Biophys. Res. Commun. **312:**1159–1164.
48. **Yang, Z. Y., Y. Huang, L. Ganesh, K. Leung, W. P. Kong, O. Schwartz, K. Subbarao, and G. J. Nabel.** 2004. pH-dependent entry of severe acute respiratory syndrome coronavirus is mediated by the spike glycoprotein and enhanced by dendritic cell transfer through DC-SIGN. J. Virol. **78:**5642–5650.
49. **Ying, W., Y. Hao, Y. Zhang, W. Peng, E. Qin, Y. Cai, K. Wei, J. Wang, G. Chang, W. Sun, S. Dai, X. Li, Y. Zhu, J. Li, S. Wu, L. Guo, J. Dai, P. Wan, T. Chen, C. Du, D. Li, J. Wan, X. Kuai, W. Li, R. Shi, H. Wei, C. Cao, M. Yu, H. Liu, F. Dong, D. Wang, X. Zhang, X. Qian, Q. Zhu, and F. He.** 2004. Proteomic analysis on structural proteins of severe acute respiratory syndrome coronavirus. Proteomics **4:**492–504.
50. **Yuan, K., L. Yi, J. Chen, X. Qu, T. Qing, X. Rao, P. Jiang, J. Hu, Z. Xiong, Y. Nie, X. Shi, W. Wang, C. Ling, X. Yin, K. Fan, L. Lai, M. Ding, and H. Deng.** 2004. Suppression of SARS-CoV entry by peptides corresponding to heptad regions on spike glycoprotein. Biochem. Biophys. Res. Commun. **319:**746–752.
51. **Zhu, J., G. Xiao, Y. Xu, F. Yuan, C. Zheng, Y. Liu, H. Yan, D. K. Cole, J. I. Bell, Z. Rao, P. Tien, and G. F. Gao.** 2004. Following the rule: formation of the 6-helix bundle of the fusion core from severe acute respiratory syndrome coronavirus spike protein and identification of potent peptide inhibitors. Biochem. Biophys. Res. Commun. **319:**283–288.